

PHASE STABILITY ISSUES IN EMERGING TBC SYSTEMS

Noemí R. Rebollo, Ashutosh S. Gandhi and Carlos G. Levi

University of California, Santa Barbara

Materials Department, Engineering II

Santa Barbara, CA 93106-5050

ABSTRACT

The high temperature stability of metastable single-phase zirconias co-doped with Y plus trivalent rare earth cations is discussed. The motivation arises from strategies to enhance the insulating efficiency and/or higher temperature capability of thermal barrier systems by co-doping the conventional ZrO_2 -7.6% $\text{YO}_{1.5}$ composition. The fundamental issue is the resistance to partitioning of the metastable tetragonal (t') or cubic (c') phases into the equilibrium assemblage dictated by the phase diagram, whereupon the stabilizer-depleted tetragonal phase becomes susceptible to the disruptive monoclinic transformation. The experiments rely on compositions synthesized by precursor pyrolysis, all of which yield initially supersaturated single-phase solid solutions. Clear trends are noted in the phase stability of single and co-doped compositions, which increases with decreasing the size of the rare earth cation. Thermodynamic arguments are offered to rationalize these trends, with additional comments on the potential roles of diffusion and clustering phenomena.

INTRODUCTION

Zirconias co-doped with yttria and one or more rare earth oxides (REO) offer potential benefits in reducing the thermal conductivity of thermal barrier coatings (TBCs) below current levels [1, 2]. In general, these materials are based on REO additions to the standard ~ 7.6 mole% $\text{YO}_{1.5}$ partially stabilized zirconia (7YSZ), and occur as metastable single phases instead of the tetragonal + cubic assemblage expected from the equilibrium phase diagram (Fig. 1). In this metastable condition, the material can be thermally cycled without undergoing the disruptive tetragonal-monoclinic transformation that compromises the mechanical integrity of the coating. Because this transformation is generally diffusionless, “non-transformability” requires selecting a coating composition whose $T_0(t/m)$ temperature is below ambient. However, prolonged exposure to high temperature ($\geq 1200^\circ\text{C}$) drives the microstructure to its equilibrium two-phase configuration [3], yielding a Y-depleted tetragonal form whose $T_0(t/m)$ is now above ambient (Fig. 1). This renders the coating “transformable” to monoclinic degrading the tolerance of the coating to thermal cycling. In this context, “phase stability” reflects the resistance of the coating material to this partitioning process at high temperature, and is thus a requisite (albeit not sufficient) condition for TBC durability in gas turbine applications. The present investigation aims to evaluate and understand the effects of rare earth co-doping on the high temperature stability of the t' phase, using the standard 7YSZ material as a baseline.

Published in “High Temperature Corrosion and Materials Chemistry IV

“ E. Opila, P. Hou, T. Maruyama, B. Pieraggi, M. McNallan, D. Shifler, and E. Wuchina (eds.)

Electrochemical Society Proceedings vol. PV-2003-16, pp. 431-442 (2003)..

EXPERIMENTAL

Two groups of materials based on 7YSZ were investigated. In one the Y was fully replaced by a RE cation and the stabilizer content was kept constant at 7.6% $\text{MO}_{1.5}$. In the other, 7.6% REO (or yttria) was added to the standard 7YSZ, bringing the total stabilizer content to 15.2%. All compositions were synthesized by reverse co-precipitation of precursor powders from mixed solutions containing the requisite cations [4]. Starting materials were Zr acetate solution in dilute acetic acid (Aldrich) and RE nitrates in powder form (Alfa Aesar), with a minimum purity of 99.9%. The nitrates were prepared as aqueous stock solutions, assayed for oxide content, and then mixed with the Zr acetate solution in the proportions needed to yield the desired compositions. Precipitation was effected by drop-wise addition of the mixed solution to aqueous NH_4OH ($\text{pH} = 9$). This approach is more effective than straight co-precipitation (i.e. by adding the base to the precursor solution) when homogeneity of the powders is a concern [4]. The precipitates were dried and pyrolyzed at 900°C for 2 h yielding single-phase supersaturated solid solution powders. The crystallite size, calculated by the Scherrer method [5, 6] was reasonably constant for all pyrolyzed powders: ~ 31 nm on average with a standard deviation of ~ 4 nm.

Specimens were heat treated primarily as loose particulate, without compaction, to minimize constraint effects that may hinder the tetragonal-monoclinic transformation. (Comparative studies with compacted and coating specimens of selected compositions are underway to evaluate these effects.) The heat treatment schedule consisted of 24 h cycles, the first four at 1200°C with increments of 50°C in each subsequent cycle. For these treatments the samples were (i) placed within a covered crucible, (ii) introduced into a furnace pre-heated to the prescribed temperature, (iii) held isothermally for 24h and, (iv) withdrawn to cool in air. Phase analysis by X-ray diffraction at room temperature was performed after each cycle, with Raman spectroscopy in selected cases. The approximate fraction of monoclinic was estimated from:

$$X_m = \frac{I(\bar{1}11)_m + I(111)_m}{I(\bar{1}11)_m + I(111)_m + I(111)_{t/c}} \quad (1)$$

wherein I is the integrated area of the (111) peak for the monoclinic (m), tetragonal (t) or cubic (c) phases. The heating schedule was designed to rank the compositions according to their resistance to de-stabilization, rather than to quantify the partitioning kinetics of a specific composition [7]. Studies of the latter type are in progress.

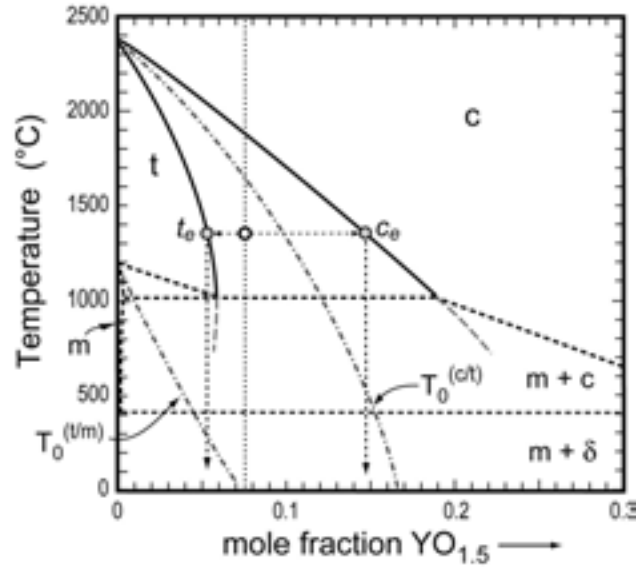


Fig. 1. Zirconia-rich end of the $\text{ZrO}_2\text{-YO}_{1.5}$ phase diagram showing the temperatures for diffusionless transformation from cubic to tetragonal, $T_0(c/t)$, and from tetragonal to monoclinic, $T_0(t/m)$. The dotted line at 7.6% represents the standard TBC composition comprising the metastable t' phase.

RESULTS AND DISCUSSION

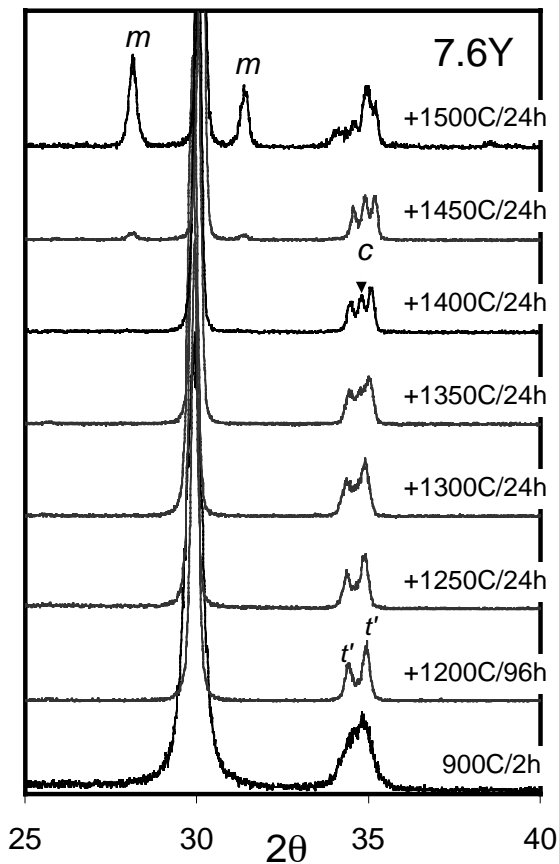


Fig. 2. XRD patterns for $\text{ZrO}_2\text{-}7.6\%\text{YO}_{1.5}$ after various stages in the heat treatment. t' denotes the (200)/(002) tetragonal peaks, c the (200) cubic peak and m the (111) monoclinic peaks.

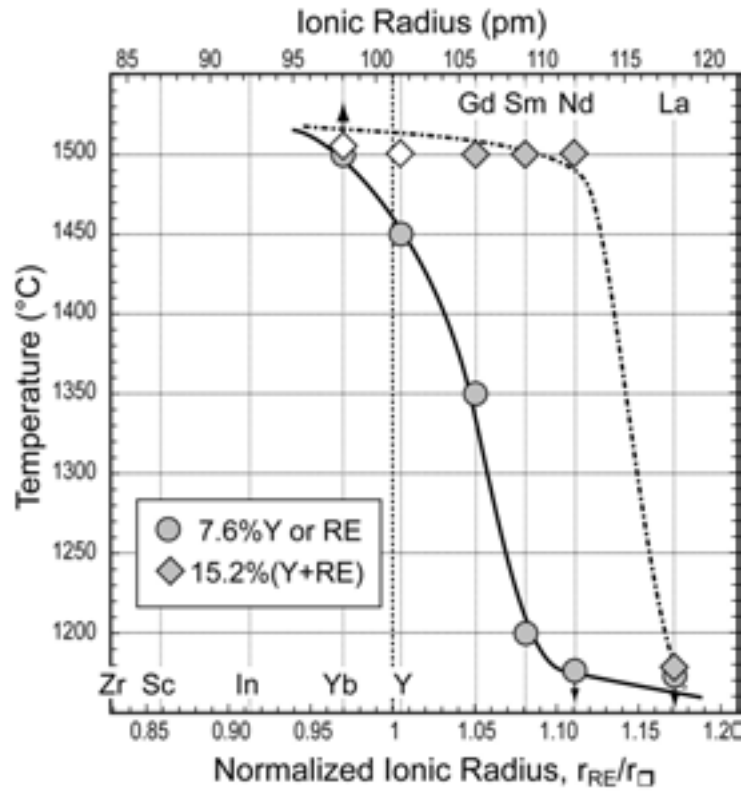
consequence of the reduction in the relative amount of equilibrium tetragonal phase with increasing temperature, and hence in the amount of monoclinic that can form from it. Since a small amount of monoclinic is presumably tolerable, the “practical” onset of destabilization was set when partitioning leads to X_m in Equation (1) to be $>10\%$. (An exception is the La co-doped 7YSZ, wherein extensive partitioning is observed but no evidence of monoclinic is detected, as discussed later.)

Singly Doped Compositions

The temperature of the heat treatment stage immediately prior to “substantial” partitioning, e.g. 1450°C in Fig. 2, is designated as the “stability limit” for the purposes of the present comparison. These temperatures are plotted in Fig. 3 for the two groups of materials investigated. It is evident in this figure that the effectiveness of a single dopant in preserving t' stability decreases systematically with increasing ionic size within the range studied. All materials exhibit essentially the same XRD pattern in the as-pyrolyzed condition (cf. Fig. 2), with La showing the least evidence of tetragonality. Only the slightest hint of monoclinic was detectable at the highest temperatures for the 7.6Yb composition, whereas materials based on Nd and La partitioned extensively during the first 24h cycle at 1200°C (i.e. their “stability limit” would be below the range investigated). In both Nd and La the products of partitioning were the pyrochlore zirconate and

Results for powders of the baseline 7YSZ material are given in Fig. 2. Because of their fine crystallite size (~ 30 nm), it is not immediately obvious whether the powders after pyrolysis are tetragonal or cubic. Their single phase nature, however, is conclusively ascertained from the XRD pattern after the first 24h cycle at 1200°C (not in Fig. 2), which clearly shows the peaks characteristic of single-phase $t\text{-ZrO}_2$. Evidence of supersaturation is provided by the appearance of a (200) cubic peak between the (200)/(002) tetragonal peaks in the patterns for 1350-1450°C in Fig. 2. It is noted that monoclinic does not appear concurrently with the first observation of this cubic peak, presumably because the associated depletion of Y from the t' phase is still insufficient to render it transformable. (The absence of $m\text{-ZrO}_2$ at these temperatures was confirmed by Raman spectroscopy.) At some point small monoclinic peaks may appear, e.g. after 1450°C in Fig. 2. These may develop fully in the next stage of the heat treatment (1500°C), but in other compositions they grow only slightly and may even disappear at higher temperatures. The latter is a consequence of the reduction in the relative amount of equilibrium tetragonal phase with increasing temperature, and hence in the amount of monoclinic that can form from it. Since a small amount of monoclinic is presumably tolerable, the “practical” onset of destabilization was set when partitioning leads to X_m in Equation (1) to be $>10\%$. (An exception is the La co-doped 7YSZ, wherein extensive partitioning is observed but no evidence of monoclinic is detected, as discussed later.)

Fig. 3. Relative resistance to de-stabilization in the systems investigated, plotted as the temperature of the last heat treatment stage before the onset of substantial monoclinic formation, as a function of ionic size (8-fold coordination) [8]. The normalization length scale, r_{\square} , is the radius of the interstitial “cubic” site coordinated by 8 oxygen anions. The circles represent singly doped compositions (Y or rare earth), while the diamonds represent ternary compositions containing equal proportions of Y and a RE dopant, with the 15.2%YO_{1.5} composition added for comparison. The empty symbols denote compositions that did not exhibit any signs of partitioning. The radii of Sc and In, two alternate trivalent stabilizers, are given for reference.



tetragonal zirconia, subsequently transformed to monoclinic. Sm and Gd behaved qualitatively like Y, except for the lower stability temperature and the absence of the pre-transition (200) cubic peak.

The reasons for the trend of decreasing stability with ionic size are not immediately evident. The decomposition of t' into the equilibrium tetragonal + cubic forms requires long-range cation diffusion. Since the host structure is the same and the nature of the rate-controlling defects for cation diffusion [9] is expected to be similar, one may argue that the diffusion rates should vary inversely with cation size. The implication is that phase stability would increase with increasing dopant size, which is clearly at variance with the experimental observations. Conversely, the phase equilibria information on these systems, albeit limited and still in need of verification, suggests the driving force may also change systematically with ionic size.

Figure 4 shows tentative binary diagrams for ZrO₂ and Lanthanide oxides, including YO_{1.5} for comparison. Notable are the systematic trends with decreasing ionic size, including the increase in the extent of the cubic (fluorite) field and the associated $t + c$ equilibrium, as well as the decrease in the stability of the pyrochlore zirconate M₂Zr₂O₇. The ZrO₂-YO_{1.5} diagram fits very well within this trend if placed according to ionic size, but not if placed according to atomic number/mass (smaller than La). Two different groups can be identified in the context of the problem at hand. One comprises Sm, Gd, Y and Yb, wherein de-stabilization involves the precipitation of cubic phase from the supersaturated t' at all temperatures of interest (1200-1500°C). The other group includes La and Nd, which would tend to precipitate the zirconate instead of the cubic phase to relieve the supersaturation of t' , albeit only at the lower temperatures in the case of Nd.

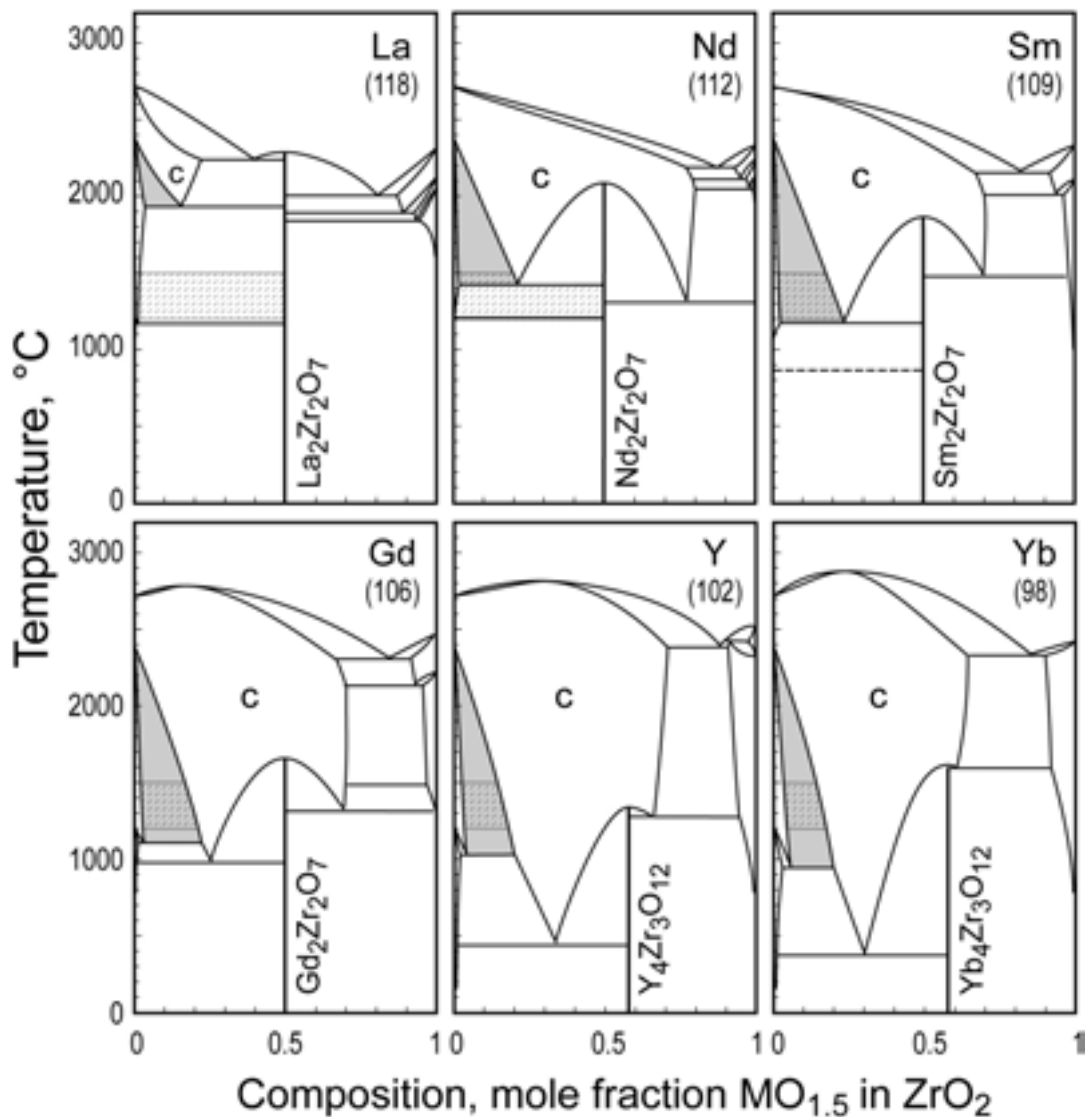


Fig. 4. Binary phase diagrams for the stabilizers investigated, in order of decreasing ionic size, adapted from calculations by Yokokawa [10]. The S-P ionic sizes are indicated in parenthesis. The tetragonal + cubic field is shaded in gray. The hatched region represents the relevant two-phase fields and temperature range for the materials investigated. Note the well behaved trend in phase equilibria including that pertaining to Y, which does not belong to the Lanthanide period but fits the trend based on ionic size.

It can be shown that the maximum driving force for the separation of t' into $t + c$ increases with the width of the corresponding two-phase field [7]. Prior reports in the literature [11, 12] suggest that the $t + c$ field widens systematically from Y to Nd. The inference is that the driving force for phase separation may increase with increasing ionic size, as elaborated below. It is noted, however, that there are inconsistencies between the cited studies and the $t + c$ boundaries are still under debate, even for Y. Notably, the equilibrium tetragonal boundaries in [11] exhibit a retrograde shape with a maximum in solid solubility at temperatures much higher than those suggested by more comprehensive phase diagram evaluations, e.g. [13, 14] for Y—cf. Fig. 1.

In the context of the problem at hand, the phase diagram information may be cast in the form of two distinct thermodynamic scenarios, illustrated in Fig. 5. The baseline is

the $\text{ZrO}_2\text{-YO}_{1.5}$ system, for which assessed Gibbs free energy descriptions of the relevant phases are available—curves marked Y in Fig. 5(a). The width of the two-phase field is determined by the common tangent, in the usual fashion, and the overall driving force for partitioning is the distance between the tetragonal free energy curve, $G(t)$, and the point on the common tangent corresponding to the same composition. The structural model for oversized trivalent dopants in ZrO_2 includes 8-fold coordination for the dopant with the anion vacancies located preferentially in the vicinity of Zr ions to relieve the “oxygen crowding” around them [15-17]. The dopant is compressed by the surrounding lattice [16] owing presumably to its size difference with Zr (from ~16% for Yb to ~40% for La). Arguably, the associated strain energy in the lattice may induce the free energy vs. composition curve to rise faster for a larger cation, as illustrated schematically for Gd in Fig. 5(a). In consequence, the equilibrium tetragonal and cubic compositions would shift to lower and higher value, respectively, relative to Y, reflecting the widening of the two-phase field with increasing cation size discussed above [11].¹ More importantly, the driving force for de-stabilization would likely increase as the intersection of the free energy curves shifts upward with increasing ionic size (inset in Fig. 5a).

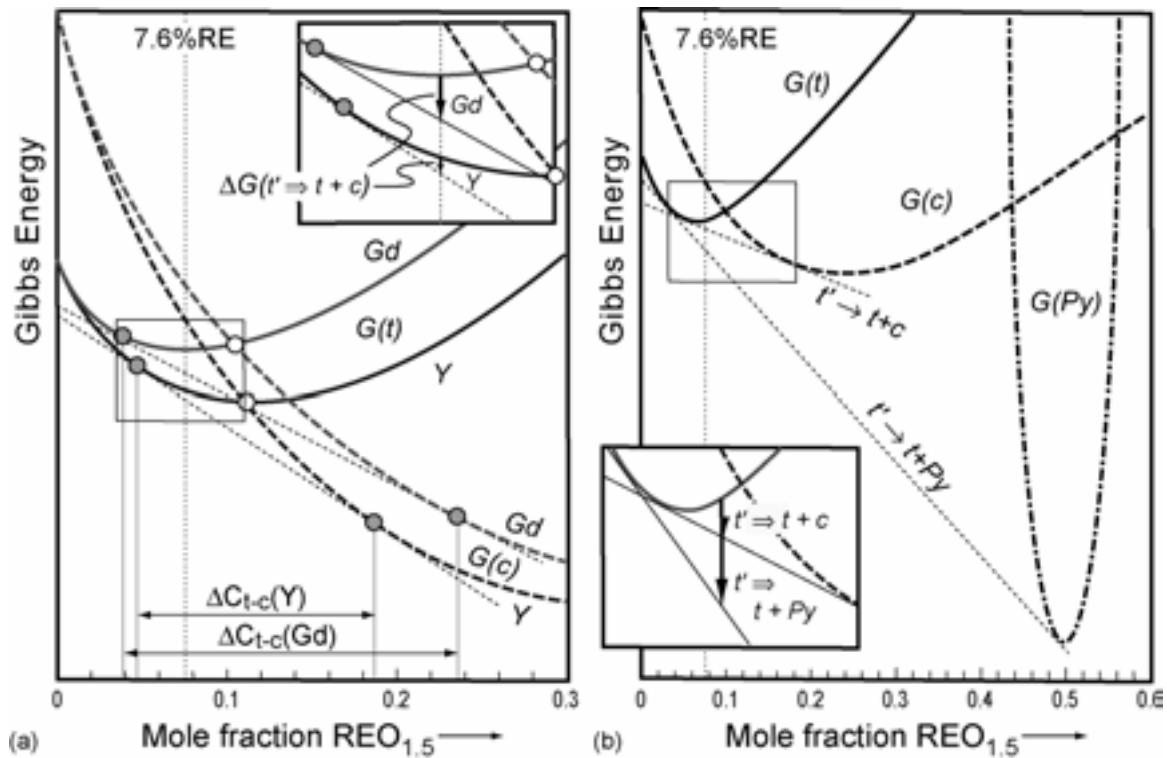


Fig. 5. Schematic Gibbs free energy curves showing the thermodynamic scenarios that may account for differences in the driving force for partitioning among the systems investigated. The curves for the $\text{ZrO}_2\text{-YO}_{1.5}$ system were calculated from revised thermodynamic models for the cubic and tetragonal phases developed by Fabrichnaya [14]. The rest of the curves are schematic, drawn to be qualitatively consistent with the phase diagrams and the expected effects of ionic size on the free energy of the relevant phases.

¹ Katamura et al. [11] proposed a continuous free energy curve wherein the tetragonal form is viewed as an “ordering” of the oxygen lattice relative to the cubic array in ideal fluoride. The difference is not significant for the purposes of the present discussion, but may become an issue in elucidating the partitioning mechanism.

For systems in which the pyrochlore is preferred over cubic as the precipitate from a supersaturated tetragonal phase, the difference in driving force is likely to be more substantial. The general situation is illustrated in Fig. 5(b). The relative positions of the free energy curves below the c (fluorite) $\rightarrow t + \text{Py}$ eutectoid (Fig. 4) is such that the overall driving force for pyrochlore precipitation should be significantly larger than that for the cubic phase, as inferred from the relative positions of the respective common tangents. A significant degradation in phase stability should then be expected as one moves from the systems in which the preferred precipitate is cubic (Yb, Y, Gd) to those in which it is pyrochlore (Nd, La), in agreement with the experimental results. Sm represents an intermediate case in which the lowest heat treatment temperature (1200°C) is quite close to the $c \rightarrow t + \text{Py}$ eutectoid and seems to be only marginally more stable than those compositions forming pyrochlore (Fig. 3).

A thermodynamic argument is thus more consistent with the experimental observations than one based on differences in diffusion kinetics. However, diffusion kinetics is clearly important in that it prevents partitioning at the lower temperatures (where “lower” depends on the relative driving force and hence on the dopant). Moreover, limited experiments on Y and Gd single-doped systems reveal that phase stability is enhanced by increasing composition [7], a result that cannot be fully explained with thermodynamics and requires improved understanding of the partitioning kinetics. For example, Fig. 5 shows that the driving force for partitioning at a constant temperature should increase monotonically from the tetragonal boundary to the composition corresponding to the $T_0(c/t)$ curve, and then decrease monotonically to vanish at the cubic boundary. However, the partitioning resistance of Y-doped t' increases in the order 7.6% < 11.4% < 15.2% [7]. Arguments based on reported trends on lattice cation diffusion, which decreases with increasing Y content [9] would be qualitatively consistent with the observed trend for Y, but not with the differences between dopants, as noted before.

Additional thermodynamic and kinetic considerations may also bear on the observed trends in phase stability. The discussion so far has ignored any potential influence of the dopant on the position of the $T_0(t/m)$ curve, partly because of conflicting reports in the literature regarding the relative effect of trivalent rare-earth stabilizers on the t/m equilibrium. An interesting example is that of Sc, a dopant claimed in the literature to be more effective than Y in preserving the stability of t' at higher temperature [18]. Examination of the $\text{ZrO}_2\text{-ScO}_{1.5}$ phase equilibria and metastable relationships [19] suggests that Sc could be less effective than Y at comparative stabilizer contents. A Sc-based t' would be closer to the equilibrium tetragonal boundary than that based on Y, and thus would have a smaller driving force for partitioning. However, the $T_0(t/m)$ curve for Sc penetrates further into the binary before it dives below ambient temperature [19]. The reported shift in $T_0(t/m)$ could render a 7.6%Sc composition “transformable” into monoclinic, even without partitioning. The inference is that higher Sc contents may be needed to yield a “non-transformable” composition, in qualitative agreement with experimental studies in the literature [18, 20]. A corollary would be the existence of an optimum in stability between Yb and Sc for a fixed stabilizer content of 7.6% in Fig. 3, with composition based on the larger cations being more sensitive to partitioning at high temperature and those based on the smaller cations to martensitic transformation upon thermal cycling, even if partitioning is absent. This scenario is currently under investigation.

The trends within the lanthanide series are less clear. Earlier studies on trivalent stabilizers (Yb, Er, Y, Sm, Nd) suggested that the t/m boundary, and arguably $T_0(t/m)$, were relatively dopant-insensitive [16, 21]. Indeed, a subsequent comparison between Er and Y [19] revealed little difference in the M_s curves, but these two stabilizers are very similar in size. Conversely, one study has reported a systematic increase in M_s with increasing ionic size (from Eu to La) at equivalent concentrations [12],² whereas another suggests a decrease in M_s with increasing dopant size (from Sc to Sm) [20]. An implication of the former trend would be that the depletion of stabilizer tolerable before rendering the t' "transformable" is smaller for the larger cations. This would be consistent with the appearance of the (200) cubic peak (reflecting the early stages of phase separation) without concurrent monoclinic evolution for Y and Yb, but not for the larger cations in this study. More reliable data on the $M_s/T_0(t/m)$ dependence on dopant size and composition is clearly needed to elucidate this issue.

Ongoing studies are also considering the potential roles of coherency in the early stages of precipitation, and clustering/ordering within the tetragonal phase prior to the onset of actual precipitation. In both cases one would anticipate that cation size differences are again important. Theoretical and experimental studies [16, 22] suggest the anion vacancies tend to cluster and order as dopant concentration increases, and the dopant cations would, if mobility allows, tend to reside near (but not next to) the anion vacancies. Two types of distortion could then disrupt the regularity of the anion shift pattern in the tetragonal structure, one associated with the vacancies and another with the compression around the larger dopant cations. Both may be envisaged as promoting the cubic over the tetragonal form, whereupon clustering could be envisaged as crating "embryos" which may provide nucleation sites for precipitation and de-stabilization of t'. (This view is supported by the emergence of pyrochlore as the preferred precipitate in the systems with larger cations, since ordering in this structure allows for more effective accommodation of the cation size differential.) Increasing ionic size does not affect the vacancy contribution, but does increase the local distortion of the anion lattice and thus the environment of the neighboring host cations. Hence, clustering effects that promote precipitate nucleation and eventual de-stabilization may become more pronounced with increasing cation size.

Co-doped Compositions

The trend for co-doped compositions in Fig. 3 is qualitatively consistent with that of the single-doped systems, with some important differences. Notably, the addition of La to 7YSZ substantially degrades its phase stability, with strong evidence of decomposition after the first 24h cycle at 1200°C. This is clearly at variance with the behavior of the smaller cation systems, in which addition of the rare earth while keeping constant the concentration of Y (7.6%) generally improves stability. Indeed, no evidence of decomposition was observed in the Yb and Y systems under the present heat treatment sched-

² Most of the compositions in [12] appear to be phase separated and thus the plots of M_s vs. concentration reported are unlikely to represent the true M_s curve because they are plotted against bulk compositions, rather than the composition of the tetragonal fraction which undergoes the partitionless transformation. Nevertheless, the trend with ionic size extends to the lowest concentrations studied (~1%MO_{1.5}), where partitioning, if present, would introduce only a small error in the concentration.

ule, and only marginal amounts of monoclinic (that decreased with treatment at higher temperatures) were detected in Gd, Sm and Nd. The latter is particularly interesting because of the contrast with La, which yields poor phase stability both alone and in combination with an equal amount of Y, whereas Nd is ineffective by itself but shows acceptable behavior in the co-doped material. A second important difference is that, while partitioning was observed in the first 1200°C cycle for the La co-doped composition, no evidence of monoclinic was detected among the products of decomposition, comprising pyrochlore, tetragonal and possibly cubic zirconia.

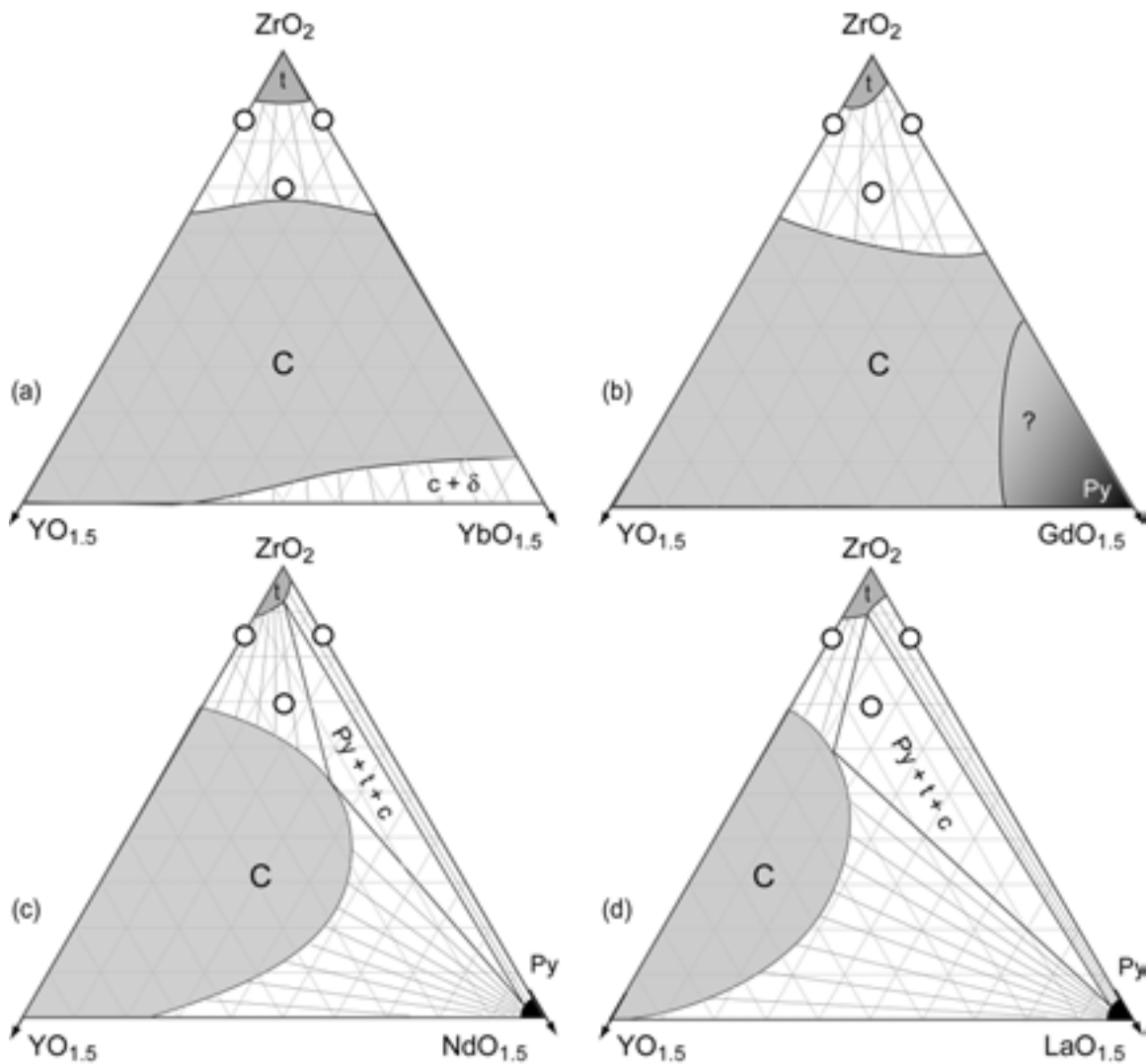


Fig. 6. Schematic ternary diagrams illustrating the different scenarios that arise when adding RE oxides to 7.6%YSZ. The temperature of the ternary sections is 1200°C. The Yb ternary is adapted from [26]. All others are schematics derived from the binaries in Fig. 4, the knowledge that there are no ternary compounds in these regions and the experimental information generated in this study. They should be taken only as qualitative approximations in need of experimental and/or theoretical validation. The $c + \text{Py}$ equilibrium in (b) is drawn to reflect gradual ordering within the fluorite field, but could also comprise a two-phase field. Note the gradual recession of the fluorite field with increasing cation size, which results in the development of binary and ternary fields where precipitation of pyrochlore is viable.

The observations can be interpreted again, albeit qualitatively, with thermodynamic arguments as illustrated by the schematic ternary diagrams in Fig. 6. For the smaller pyrochlore-forming cations (e.g. Gd, Sm) the binaries are quite similar to that with Y (cf. Fig. 4) and the fluorite field should extend across the ternary section as illustrated in Fig. 6(b). Yb does not form a pyrochlore but rather a δ ($\text{Sc}_4\text{Zr}_3\text{O}_{12}$ type) phase like Y and hence the fluorite (c), δ and $c + \delta$ fields extend similarly across the ternary (Fig. 6a), with the fluorite field being somewhat wider for the Y binary because of the lower stability of the Y zirconate (Fig. 4). The exact form of the cubic-Py equilibrium in $\text{ZrO}_2\text{-GdO}_{1.5}$ (and possibly $\text{ZrO}_2\text{-SmO}_{1.5}$) is under debate, with some studies assuming two phases with distinctly different compositions (e.g. Fig. 4) whereas others suggest the pyrochlore may be a continuous ordering domain within the fluorite field [23-25]. Figure 6(b) is drawn to illustrate the latter possibility, but the difference is not critical for the compositions investigated in the present study.

The ternary compositions with Yb, Gd and Sm are closer to the equilibrium phase boundary for the cubic phase than the singly doped materials, so that the driving force for precipitation would be smaller. The materials are likely to be metastable cubic at high temperature whereupon decomposition would occur by precipitation of the tetragonal phase. As temperature increases, the cubic boundary moves toward the ZrO_2 corner (cf. Fig. 4), and eventually the ternary composition would find itself in the equilibrium single-phase fluorite field, whereupon phase stability ceases to be an issue. Results for Y + Yb suggest that this may occur at temperatures below 1500°C . Increasing cation size toward Gd and Sm shifts the cubic boundary away from the ZrO_2 corner at any given temperature, increasing the sensitivity of the co-doped composition to de-stabilization. Materials co-doped with Gd and Sm exhibited adequate stability in the present thermal cycling schedule, but de-stabilization could certainly occur at longer times.

The fluorite phase is not stable at 1200°C in the binary systems with Nd and La, as noted before. The cubic field may then extend only partially into the ternary, as shown in Figs. 6(c) and (d), giving rise to a three-phase tetragonal (t) + cubic (c) + pyrochlore (Py) field. However, a significant difference is expected between La, where the eutectoid temperature ($\sim 2000^\circ\text{C}$) is well above the treatment range in the study, and Nd, where it is $< 1500^\circ\text{C}$ (Fig. 4). The inference is that the fluorite field in La penetrates much less into the ternary and the three-phase field is broader than in the Nd system (Figs. 6c, d). The results suggest that the ternary Y + La composition is within the three-phase (Py + t + c) field at 1200°C , whereas the Y + Nd composition falls within the t + c field. By extension of the arguments developed for the binary systems, the compositions where pyrochlore is a viable phase (La) are likely to be more prone to de-stabilization than those wherein the cubic phase is the only feasible precipitate (Nd). As temperature increases the fluorite field for Nd bridges across the ternary much earlier than that for La, further enhancing the relative stability of the former.

Analogous to the discussion of the binary materials, there may be coherency and clustering effects that affect the stability of these ternary compositions against partitioning and monoclinic transformation. It is also unclear at this point why the tetragonal phase resulting from the partitioning of t' in the La + Y co-doped compositions does not transform to monoclinic upon cooling. If the composition of the tetragonal phase were near equilibrium, this would imply that the $T_0(t/m)$ surface at ambient is closer to the ZrO_2 corner than the equilibrium tetragonal boundary at 1200°C for co-doped composi-

tions, reversing the relative positions expected in the binaries. At this point, however, there is insufficient information to assess this hypothesis. Research aimed to address these issues is currently in progress.

CONCLUDING REMARKS

Significant progress has been made in the assessment and understanding of the effects of rare earth additions ranging from Yb to La on the phase stability of t' zirconia. In binary metastable solutions of equivalent concentration and under the conditions of the present experiments, there is a clear trend wherein the resistance to partitioning and subsequent monoclinic transformation increases with decreasing size of the dopant cation. The trend includes Y, which is not part of the Lanthanide period but fits in the range of ionic sizes investigated. The differences in stability are less marked when the rare earths are added as co-dopants to Y, except for the case of La which exhibits poor performance in both cases, experiencing extensive partitioning at temperatures below 1200°C. Thermodynamic arguments are very useful in explaining the differences among dopants, but are not sufficient to elucidate all observations. Additional understanding is needed of the effects of different dopants on diffusional kinetics as well as clustering phenomena that may influence the nucleation of the second phase. Research on these issues is continuing.

ACKNOWLEDGMENTS

This investigation was sponsored by a program of international research collaboration between the National Science Foundation (DMR-0099695) and the European Commission (GRD2-200-30211) and by the Department of Energy through the Advanced Gas Turbine Research Program (Contract No: 01-01-SR093). Additional support for N.R.R. through a CONACyT/UC-MEXUS scholarship is gratefully acknowledged. The authors would like to thank Dr. Olga Fabrichnaya (Max Planck Institut für Metallforschung, Stuttgart) for useful discussions, and for making results of her ZrO₂-YO_{1.5} phase diagram evaluation available prior to publication. Interactions with MPI-MF were greatly enhanced by support for C.G.L.'s sabbatical through a Senior Research Award from the Humboldt Foundation.

REFERENCES

1. D. Zhu and R.A. Miller, *Ceramic Engineering and Science Proceedings*, **23** (4), 457, (2002).
2. J.R. Nicholls, K.J. Lawson, A. Johnstone, and D.S. Rickerby, *Surf. Coat. Technol.*, **151-152**, 383 (2002).
3. R.A. Miller, J.L. Smialek, and R.G. Garlick, in *Science and Technology of Zirconia*, A.H. Heuer and L.W. Hobbs, Editors, p.241, The American Ceramic Society Inc., Columbus, OH (1981).
4. M. Ciftcioglu and M.J. Mayo, in *Superplasticity in Metals, Ceramics and Intermetallics/1990*, M.J. Mayo, M. Kobayashi, and J. Wadsworth, Editors, Mat. Res. Soc. Symp. Proc. vol. 196, p.77, Materials Research Society, Pittsburgh PA (1990).
5. H.K. Schmid, *J. Am. Ceram. Soc.*, **70**(5), 367(1987).

6. H.P. Klug and L.E. Alexander, *X-ray diffraction procedures*, New York, NY Wiley (1974).
7. N.R. Rebollo, O. Fabrichnaya, and C.G. Levi, *Zeitschrift für Metallkunde*, **94**(3), 163 (2003).
8. R.D. Shannon and C.T. Prewitt, *Acta Crystallogr.*, **B26**(7), 1046 (1970).
9. F.R. Chien and A.H. Heuer, *Phil. Mag. A*, **73**(3), 681 (1996).
10. H. Yokokawa, N. Sakai, T. Kawada, and M. Dokiya, in *Science and Technology of Zirconia V*, S.P.S. Badwal, M.J. Bannister, and R.H.J. Hannink, Editors., p. 59, Technomic Publishing, Lancaster, PA (1990).
11. J. Katamura, T. Seki, and T. Sakuma, *J. Phase Equilibria*, **16**(4), 315 (1995).
12. E.R. Andrievskaya and L.M. Lopato, *J. Mater. Sci.*, **30**, 2592 (1995).
13. Y. Du, Z. Jin, and P. Huang, *J. Am. Ceram. Soc.*, **74**(7), 1569 (1991).
14. O. Fabrichnaya and F. Aldinger, *Thermodynamic assessment of the ZrO_2 - Y_2O_3 - Al_2O_3 system (unpublished work)* (2002).
15. S.-M. Ho, *Mater. Sci. Engng.*, **54**, 23(1982).
16. P. Li, I.-W. Chen, and J.E. Penner-Hahn., *J. Am. Ceram. Soc.*, **77**(1), 118 (1994).
17. S. Fabris, A.T. Paxton, and M.W. Finnis., *Acta Mater.*, **50**, 5171 (2002).
18. R.L. Jones and D. Mess, *Surf. Coat. Technol.*, **86-87**, 94 (1996).
19. M. Yashima, M. Kakihana, and M. Yoshimura, *Solid State Ionics*, **86-88**(pt. 2), 1131 (1996).
20. F. Boulc'h, L. Dessemond, and E. Djurado, *Solid State Ionics*, **154-155**, 143(2002).
21. M. Yoshimura, M. Yashima, T. Noma, and S. Somiya, *J. Mater. Sci.*, **25**, 2011 (1990).
22. S. Ostanin, A.J. Craven, D.W. McComb, D. Vlachos, A. Alavi, A.T. Paxton, and M.W. Finnis, *Phys. Rev. B*, **65**(22), 224109/1-9 (2002).
23. M.P. van Dijk, F.C. Mijlhoff, and A.J. Burggraaf, *J. Solid State Chem.*, **62**, 377 (1986).
24. T. Uehara, K. Koto, and F. Kanamaru, *Solid State Ionics*, **23**, 137 (1987).
25. S. Meilicke and S. Haile, in *Materials for electrochemical energy storage and conversion - batteries, capacitors and fuel cells*, D.H. Doughty et al, Editors, Mat. Res. Soc. Symp. Proc. vol. **393**, p. 55, Materials Research Society, Pittsburgh, PA (1995).
26. G.S. Corman and V.S. Stubican, *J. Am. Ceram. Soc.*, **68**(4),174 (1985).